

## Charmonium dissociation at high baryon chemical potential

Bo Tong and Baoyi Chen <sup>\*</sup>*Department of Physics, Tianjin University, Tianjin 300354, China*

(Received 26 June 2022; accepted 9 September 2022; published 21 September 2022)

We study charmonium dissociation in hot medium with a finite baryon chemical potential  $\mu_B$ . Charmonium bound states are dissociated in the medium by the color screening effect and the random scatterings with thermal partons, which are included in the real and imaginary parts of the potential, respectively. The  $J/\psi$  fraction in the  $c\bar{c}$  pair defined to be the quantum overlap between the wave package and the wave function of the  $J/\psi$  eigenstate decreases with time due to the complex potentials. When  $\mu_B$  is large compared with the medium temperature, the Debye mass is increased evidently. We consider the  $\mu_B$ -dependent Debye mass in both real and imaginary parts of the potential to calculate the  $J/\psi$  survival probability in the static medium and the Bjorken medium. The  $J/\psi$  survival probability is reduced evidently by the  $\mu_B$  effect at low temperatures available in the medium produced in the Beam Energy Scan experiments, while this effect is not apparent at high temperatures.

DOI: [10.1103/PhysRevC.106.034911](https://doi.org/10.1103/PhysRevC.106.034911)

### I. INTRODUCTION

Hot deconfined medium is believed to be produced in relativistic heavy-ion collisions [1,2]. Heavy quarkonium has been extensively studied to extract the properties of the hot QCD matter in nuclear collisions [3–11]. In the hot medium, the heavy quark potential is color screened by the thermal partons [12–14], which can dissociate the bound states of quarkonium. The degree of color screening depends on the densities of thermal partons represented by the medium temperature. With the increase of the temperature, different quarkonium bound states are sequentially melted due to their different binding energies. Besides, inelastic random scatterings from thermal partons can also dissociate quarkonium bound states [15–20], where heavy quark pairs are transformed from singlet to octet states. The singlet-octet transition process can be treated as an imaginary potential which reduces the normalization of the singlet states [17,21,22]. One can determine the medium temperature with the charmonium survival probability defined as the ratio of final and initial production of  $J/\psi$  during their evolution in the hot medium. Explicit quantum treatments have been developed to study the quarkonium's inner evolution in the medium, such as the Schrödinger-Langevin equation [23], which evolves the wave function of the quarkonium directly. The medium interaction is included via the screened potential and the noise term in the Hamiltonian. The Schrödinger equation model with complex potentials has also been developed [24–26]. The inner evolutions of the quarkonium are described with the Schrödinger equation when they move along different trajectories in the medium. Open quantum system models, such as the Lindblad equation [27] and the stochastic Schrödinger equation [28,29], which treat quarkonium as an open quan-

tum system with the momentum-energy exchange with the thermal medium have also been developed recently. Other semiclassical transport models have been developed to study the dissociation and recombination of quarkonium in the hot medium [30–32].

In the experiments of the Beam Energy Scan (BES), the initial energy density of the medium is much lower than the situation in AA collisions at the BNL Relativistic Heavy-Ion Collider (RHIC) and the CERN Large Hadron Collider (LHC). The effects of color screening and the parton random collisions become weaker in the heavy quark potential. However, the baryon chemical potential  $\mu_B$  in the medium produced in the BES experiments can be considerable. It changes the Debye mass and the heavy quark potential [33,34]. It is necessary to study the  $\mu_B$  effect on the evolution of charmonium in the baryon-rich medium with a low temperature and a large  $\mu_B$ . In this work, we employ the time-dependent Schrödinger equation with the complex potential to study the evolution of the charmonium wave function in the medium with high baryon chemical potential [25,35]. The Debye mass becomes larger due to the correction from the  $\mu_B$  term. This results in a weaker real potential and a larger imaginary potential of the quarkonium. The  $J/\psi$  fraction in the charm pair is more reduced after considering the  $\mu_B$  effect in the static medium and the Bjorken medium. Studying charmonium dissociation in high  $\mu_B$  medium helps us to understand the evolution of charmonium in the BES experiments.

This work is organized as follows. In Sec. II, we introduce the framework of the Schrödinger equation and the parametrized in-medium heavy quark potential. In Sec. III, the evolutions of the charmonium wave package in the static medium and the Bjorken medium are studied. Effects of the baryon chemical potential and the color screening are compared in the charmonium dissociations. In Sec. IV, a conclusion is given.

<sup>\*</sup>baoyi.chen@tju.edu.cn

## II. THEORETICAL MODEL

To describe the quantum evolutions of heavy quarkonium wave packages at finite  $\mu_B$  and  $T$ , we employ the time-dependent Schrödinger equation. Neglecting the relativistic effect in the inner motion of charmonium, we take the classical form of the Hamiltonian of charmonium. Hot medium effects are included via the in-medium heavy quark potential. As the QCD matter produced in heavy-ion collisions is close to a perfect liquid with very small viscosity, one can approximate the heavy quark potential to be a spherically symmetric potential. There is no transitions between the states with different angular momenta. We separate the radial part of the Schrödinger equation in the center-of-mass frame [25],

$$i\hbar \frac{\partial}{\partial t} \psi(r, t) = \left[ -\frac{\hbar^2}{2m_\mu} \frac{\partial^2}{\partial r^2} + V(r, T) + \frac{l(l+1)\hbar^2}{2m_\mu r^2} \right] \psi(r, t), \quad (1)$$

where  $r$  and  $t$  are the radius and the time, respectively;  $m_\mu = m_1 m_2 / (m_1 + m_2) = m_c / 2$  is the reduced mass in the center-of-mass frame; and  $m_c$  is the charm quark mass. The heavy quark potential  $V(r, T)$  depends on the temperature and the radius, which indicates that different eigenstates in the wave package experience different hot medium effects due to their geometry sizes.  $\psi(r, t) \equiv rR(r, t)$  is defined as the product of the radius and the radial part of the wave package  $R(r, t)$ . The total wave package of the heavy quarkonium is expanded as  $\Psi(r, \theta, \phi, t) = \sum_{nlm} c_{nl}(t) R_{nl}(r, t) Y_{lm}(\theta, \phi)$ , where  $Y_{lm}$  is the spherical function, and  $n, l$ , and  $m$  are the quantum numbers of charmonium states. The coefficient  $c_{nl}(t)$  is defined to be

$$c_{nl}(t) = \int R_{nl}(r) e^{-iE_{nl}t} \psi(r, t) r dr, \quad (2)$$

where  $|c_{nl}|^2$  is interpreted as the fraction of the charmonium eigenstate specified with the quantum number  $(n, l)$  in the total wave package. The charmonium eigenstates mentioned in this work are defined as the eigenstates of the vacuum Cornell potential with a string breaking at  $r = r_{D\bar{D}}$ ,

$$V_c(r) = \begin{cases} -\frac{\alpha}{r} + \sigma r, & r < r_{D\bar{D}}, \\ 2m_D - 2m_c, & r \geq r_{D\bar{D}}, \end{cases} \quad (3)$$

where the distance of string breaking  $r_{D\bar{D}}$  is determined via  $-\frac{\alpha}{r_{D\bar{D}}} + \sigma r_{D\bar{D}} = 2m_D - 2m_c$ . Masses of the  $D$  meson and the charm quark are taken as  $m_D = 1.87$  GeV and  $m_c = 1.27$  GeV [36], respectively. Fitting the masses of  $J/\psi$  and  $\psi(2s)$  given by the Particle Data Group, one can determine the values of the parameters  $\alpha = \pi/12$  and  $\sigma = 0.2$  GeV<sup>2</sup> [14]. With the in-medium heavy quark potential  $V(r, T)$ , fractions of charmonium eigenstates in the wave package change with time. The survival probability of charmonium eigenstates is connected with the evolutions of charmonium wave packages. The quantum transitions between different states have been included in the wave function evolutions.

To solve the Schrödinger equation numerically, we employ the Crank-Nicolson method. It can evolve the wave package in a straightforward manner in the spatial coordinate instead of projecting the wave package to a series of bases. The numerical errors of the wave function at different time steps are small enough and convergent when we take a small step

of time and the radius in the following discrete formula (in natural units  $\hbar = c = 1$ ),

$$\mathbf{T}_{j,k}^{n+1} \psi_k^{n+1} = \mathcal{V}_j^n, \quad (4)$$

where  $j$  and  $k$  are the indexes of rows and columns in the triangular matrix  $\mathbf{T}$ . The nonzero elements in the matrix are

$$\begin{aligned} \mathbf{T}_{j,j}^{n+1} &= 2 + 2a + b\mathcal{V}_j^{n+1}, \\ \mathbf{T}_{j,j+1}^{n+1} &= \mathbf{T}_{j+1,j}^{n+1} = -a, \\ \mathcal{V}_j^n &= a\psi_{j-1}^n + (2 - 2a - b\mathcal{V}_j^n)\psi_j^n + a\psi_{j+1}^n, \end{aligned} \quad (5)$$

where  $a = i\Delta t / (2m_\mu(\Delta r)^2)$  and  $b = i\Delta t$ . Here  $i$  is an imaginary unit. The subscript  $j$  and the superscript  $n$  represent the coordinate  $r_j = j \cdot \Delta r$  and  $t_n = n \cdot \Delta t$ , respectively. The steps of the radius and the time are taken to be  $\Delta r = 0.03$  fm and  $\Delta t = 0.001$  fm/c. The numerical accuracy in the evolution of the wave package is high enough when taking these parameters. The time dependence in the potential comes from the time evolution of the temperature. In the static medium with a constant temperature, the potential does not depend on time anymore. At each time step, we calculate the inverse of the matrix  $\mathbf{T}$  with the Gauss-Jordan element elimination method in Eq. (4) to obtain the wave package at the next time step  $\psi^{n+1} = [\mathbf{T}^{n+1}]^{-1} \cdot \mathcal{V}^n$ . The fractions of charmonium eigenstates are obtained by projecting the wave package to the wave function of the eigenstate.

The realistic in-medium heavy quark potential is between the limits of the free energy  $F$  and the internal energy  $U$ . There are theoretical studies indicating that the in-medium potential is more close to the limit of  $U$  in the temperatures available in AA collisions at the RHIC and the LHC [7,37]. Considering that the internal energy  $U = F + T(-\partial F/\partial T)$  can become a bit stronger than the vacuum Cornell potential at the temperatures around  $T_c$  [25,26], which results in an oscillation behavior in the time evolution of charmonium fractions in the wave package, we take the free energy as the heavy quark potential to evolve the wave package. The real part of the potential is then parametrized with the following form [26],

$$V_R(r, T, \mu_B) = -\frac{\alpha}{r} e^{-m_d r} + \frac{\sigma}{m_d} (1 - e^{-m_d r}), \quad (6)$$

where the Debye mass  $m_d(T, \mu_B)$  depends on the temperature and the baryon chemical potential  $\mu_B$  [33],

$$\begin{aligned} m_d(T, \mu_B) &= T \sqrt{\frac{4\pi N_c}{3} \alpha \left(1 + \frac{N_f}{6}\right)} \\ &\times \sqrt{1 + \frac{3N_f}{(2N_c + N_f)\pi^2} \left(\frac{\mu_B}{3T}\right)^2}, \end{aligned} \quad (7)$$

where the factors of color and flavor are taken as  $N_c = N_f = 3$ . As we focus on the effect of baryon chemical potential  $\mu_B$  at the collision energies available in the BES experiments, the value of baryon chemical potential is estimated with the relation [38,39]

$$\mu_B(\sqrt{s_{NN}}) = \frac{1.3}{1 + 0.28\sqrt{s_{NN}}}. \quad (8)$$

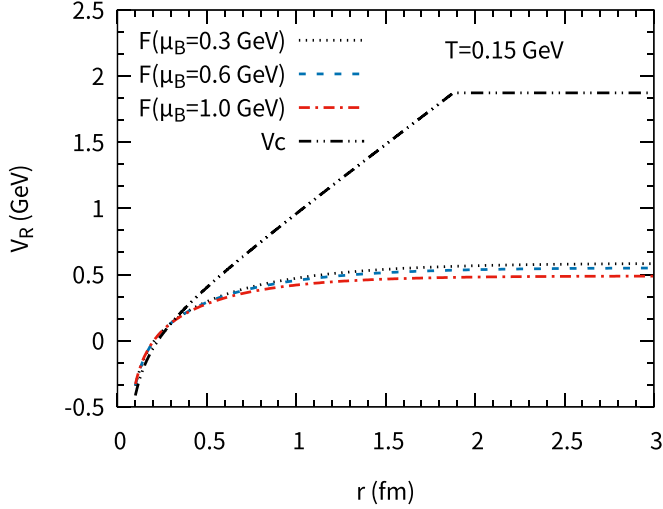


FIG. 1. The heavy quark potential as a function of the radius at different temperatures. Dotted, dashed, and dotted-dashed lines are the in-medium heavy quark potential (taken as the free energy  $F$ ) with the baryon chemical potential  $\mu_B = 0.3, 0.6,$  and  $1.0$  GeV, respectively. The temperature is taken as  $T = 0.15$  GeV. The Cornell potential is also plotted and labeled with  $V_c$ .

In order to estimate the value of  $\mu_B$  in the BES experiments, we choose  $\sqrt{s_{NN}} = 10$  GeV to get a value of the baryon chemical potential of  $\mu_B \approx 0.3$  GeV. The value of  $\mu_B$  can be larger than the medium temperature in the collisions of the BES experiments. The Debye mass is increased by the term with  $\mu_B/(3T)$ . In the following calculations, we take different values of  $\mu_B$  to check the  $\mu_B$  effect. The color-screened potential at finite  $\mu_B$  is plotted in Fig. 1.

Random inelastic scatterings with thermal partons can also dissociate quarkonium bound states in the medium, which contributes an imaginary part in the potential of the singlet states. We take the parametrization based on the calculation from hard thermal loop resummed perturbation theory [40,41],

$$V_I(r, T, \mu_B) = -i \frac{g^2 C_F T}{4\pi} \tilde{f}(\hat{r}), \quad (9)$$

$$\tilde{f}(\hat{r}) = 2 \int_0^\infty dz \frac{z}{(z^2 + 1)^2} \left[ 1 - \frac{\sin(z\hat{r})}{z\hat{r}} \right], \quad (10)$$

where  $i$  is the imaginary unit;  $C_F = (N_c^2 - 1)/(2N_c)$ ; and  $\hat{r} \equiv rm_d(T, \mu_B)$  is the dimensionless variable. The coupling constant is  $g = \sqrt{4\pi\alpha N_c/3}$ . The value of  $\alpha$  is taken as the same as with the Cornell potential. With this form, the  $\mu_B$  effect in  $V_I$  is included via the Debye mass. The magnitude of  $V_I/T$  with different values of  $\mu_B$  is plotted in Fig. 2.

### III. NUMERICAL RESULTS

To study the effects of the baryon chemical potential on the evolution of the charmonium wave package, we take different values of  $\mu_B$  in the calculations. The initial wave package is initialized with the wave function of  $J/\psi$ . In Fig. 3, the temperature of the static uniformly-distributed medium is  $T = 0.15$  GeV. With only the real part of the potential

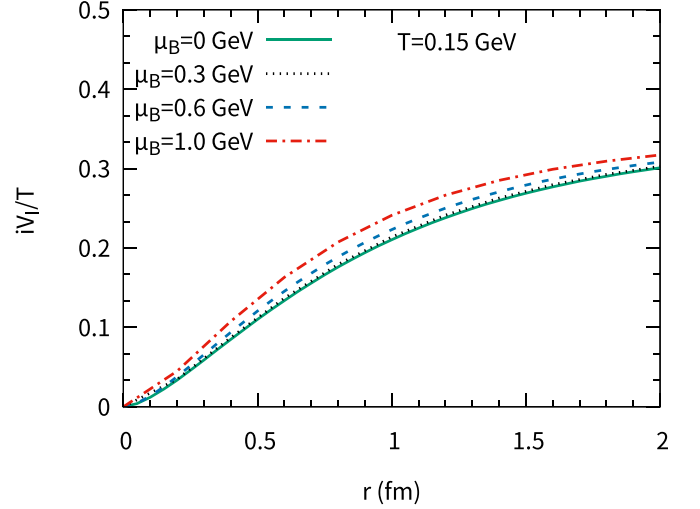


FIG. 2. The imaginary part of the potential scaled with the temperature  $iV_I/T$  as a function of the radius. Dotted, dashed, and dotted-dashed lines with different values of  $\mu_B = (0, 0.3, 0.6, 1.0)$  GeV are plotted, respectively. The temperature is taken as  $T = 0.15$  GeV.

in Fig. 3, the wave package expands outside, which reduces the quantum overlap between the charmonium wave package and the wave function of the  $J/\psi$  state. As the geometry size of the excited state  $\psi(2S)$  is larger than the size of the  $J/\psi$  wave function, the quantum overlap between the wave package and the  $\psi(2S)$  wave function increases with time, shown as the lines in Fig. 3. This behavior corresponds to the transitions of  $J/\psi$  to  $\psi(2S)$  components in the wave package. The Debye mass with the baryon chemical potential  $\mu_B = 0.6$  GeV increases about 9% compared with the case of  $\mu_B = 0$ . At high temperatures, the corrections of the  $\mu_B$  term in the

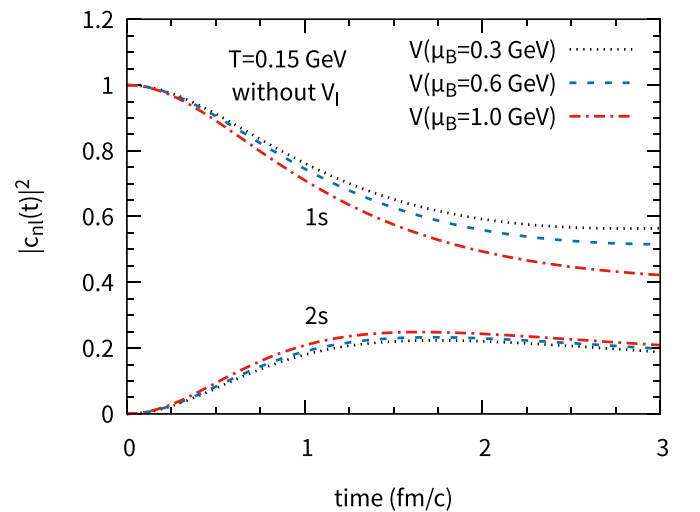


FIG. 3. The fraction of the  $J/\psi$  eigenstate in the wave package as a function of time. The baryon chemical potential is taken as  $\mu_B = 0.3, 0.6,$  and  $1.0$  GeV, respectively. Only the real part of the potential is included in the calculations. The temperature of the static medium is  $T = 0.15$  GeV.

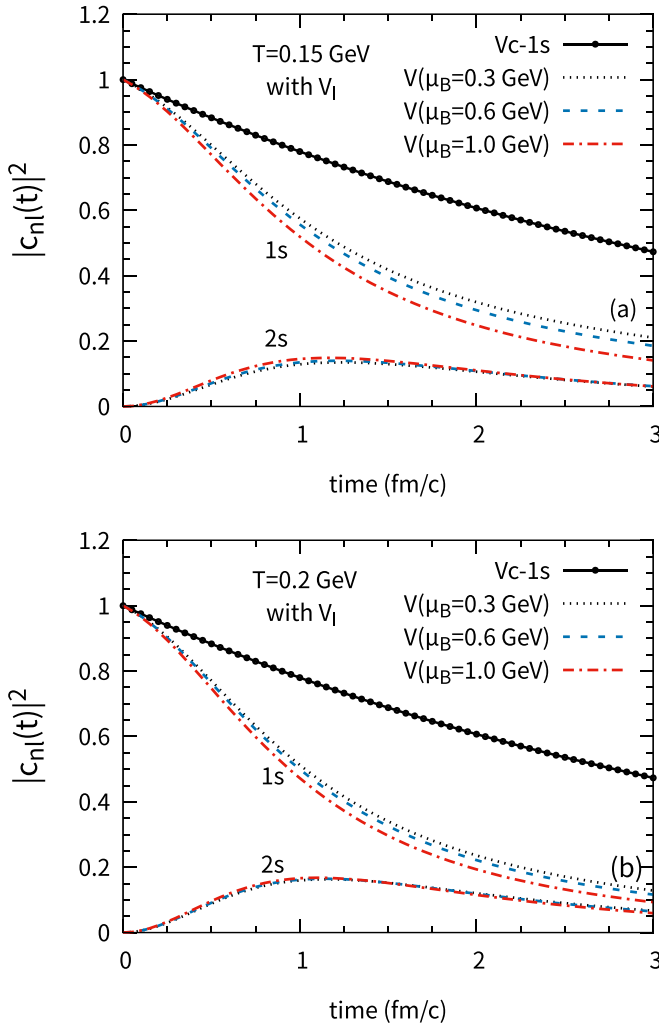


FIG. 4. The fraction of  $J/\psi$  and  $\psi(2S)$  eigenstates in the wave package as a function of time. Both real and imaginary parts of the heavy quark potential are employed. The medium temperature is taken as  $T = 0.15$  and  $0.2$  GeV, respectively [see the panels (a) and (b)]. Black solid lines with markers employ the vacuum Cornell potential plus the imaginary potential. Other parameters are the same as those in Fig. 3.

heavy quark potential become smaller. Time evolutions of the  $J/\psi$  fraction in the wave package are close to each other when taking different values of  $\mu_B$ . In Fig. 3, the sum of the fractions of  $J/\psi$  and  $\psi(2S)$  states becomes smaller than 1, as some components of the wave package transform into higher eigenstates and scattering states due to the weak attraction in the wave package.

As introduced before, the transition from singlet to octet states induced by the parton random scatterings contributes an imaginary part in the potential of the singlet states. This reduces the normalization of the total wave package. After considering the imaginary potential given by Eq. (9), we study the  $J/\psi$  survival probability in the static medium in Fig. 4. All the hot medium effects including color screening,  $\mu_B$  correction, and inelastic scatterings are included. To check the contribution of the imaginary potential, we take the heavy

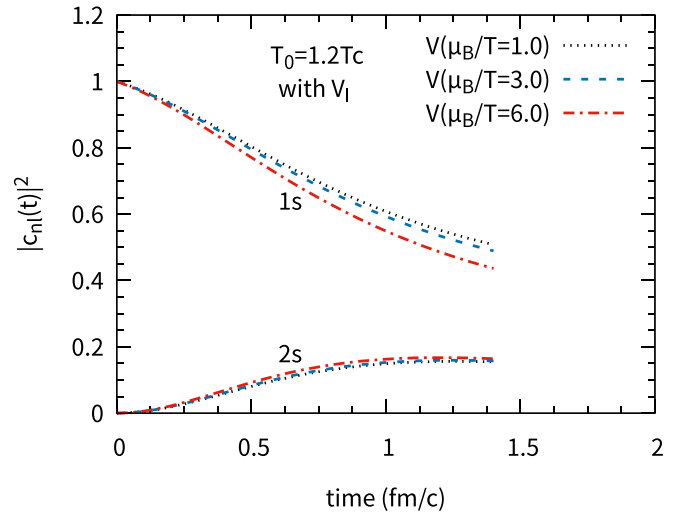


FIG. 5. The fraction of the  $J/\psi$  state in the wave package as a function of time in the Bjorken medium. The initial temperature of the medium is chosen as  $T(t_0) = 1.2 T_c$ . The starting time of the evolution is  $t_0 = 0.6$  fm/c. Dotted, dashed, and dotted-dashed lines correspond to the cases of the complex potentials  $V = F + V_I$  with  $\mu_B/T = (1.0, 3.0, 6.0)$ , respectively.

quark potential to be  $V_c + V_I(\mu_B = 0)$ , the reduction of the  $J/\psi$  fraction in the wave package is induced by the imaginary potential, shown as the black solid lines with markers in Fig. 4. When the screened potential is also employed, the  $J/\psi$  fraction is more suppressed. At the time  $t \approx 3$  fm/c, the  $J/\psi$  fraction with  $\mu_B = 1.0$  GeV is suppressed by around 25% compared with the situation of  $\mu_B = 0$  at  $T = 0.15$  GeV. This effect becomes smaller at a higher temperature of  $T = 0.2$  GeV, shown in Fig. 4(b). In the long time limit, all the bound states are dissociated by parton scatterings where the fractions of  $J/\psi$  and  $\psi(2S)$  go to zero.

In the relativistic heavy-ion collisions, hot medium is produced followed by a violent expansion. The medium temperature decreases with time. As a preliminary study, we neglect the transverse expansion of the medium and only consider the longitudinal expansion, where the temperature evolution can be characterized with the Bjorken model as follows,

$$\frac{T(t)}{T(t_0)} = \left(\frac{t_0}{t}\right)^{1/3}, \quad (11)$$

where  $t_0$  is the starting time of the Bjorken expansion. From hydrodynamic models, it is estimated to be  $t_0 = 0.6$  fm/c [42,43]. The initial temperature is chosen as  $T(t_0) = 1.2 T_c$ , which is close to the initial temperature of the medium produced in BES collisions. The Schrödinger equation evolves until the temperature becomes lower than the cut  $T_f = 0.8 T_c$  which is around the temperature of the medium kinetic freeze-out. Below this cut, the heavy quark potential is taken as the vacuum Cornell potential.

In Fig. 5, the complex heavy quark potential is taken as the free energy plus the imaginary potential. In order to fix the value of entropy per baryon density, we take the value of  $\mu_B/T = (1.0, 3.0, 6.0)$ , respectively. The Debye mass in

both real and imaginary parts of the potential depends on  $\mu_B/T$ . In Fig. 5, one can see that the  $J/\psi$  fraction is reduced by around 15% in the line with  $\mu_B/T = 6.0$  compared with the situation of  $\mu_B = 0$  at the end of the Bjorken medium evolution. The  $\mu_B$  effect can evidently reduce the charmonium survival probability in the baryon-rich medium. Note that in the dense medium, there is also Friedel oscillation in the real part of the potential [44], which may also affect the evolution of the quarkonium wave package. This effect is neglected in the work and deserves further studies in the future.

#### IV. SUMMARY

In this work, we employ the Schrödinger equation to study the evolution of the charmonium wave package at a finite

baryon chemical potential. The  $J/\psi$  fraction in the wave package is obtained by calculating the quantum overlap between the wave package and the wave function of the  $J/\psi$  eigenstate. The  $\mu_B$  correction is included in the Debye mass which is employed in both real and imaginary parts of the potential. With a large value of  $\mu_B/T$ , the  $J/\psi$  dissociation rate is enhanced in the baryon-rich medium. In following work, we will also consider the  $\mu_B$  dependence in the equation of state of the hot medium consistently.

#### ACKNOWLEDGMENT

This work is supported by the National Natural Science Foundation of China (NSFC) under Grants No. 12175165 and No. 11705125.

- 
- [1] Y. Aoki, G. Endrodi *et al.*, *Nature (London)* **443**, 675 (2006).  
 [2] A. Bazavov, T. Bhattacharya *et al.*, *Phys. Rev. D* **85**, 054503 (2012).  
 [3] T. Matsui and H. Satz, *Phys. Lett. B* **178**, 416 (1986).  
 [4] L. Grandchamp and R. Rapp, *Phys. Lett. B* **523**, 60 (2001).  
 [5] A. Andronic, P. Braun-Munzinger, K. Redlich, and J. Stachel, *Phys. Lett. B* **571**, 36 (2003).  
 [6] L. Yan, P. Zhuang, and N. Xu, *Phys. Rev. Lett.* **97**, 232301 (2006).  
 [7] Y. Liu, B. Chen, N. Xu, and P. Zhuang, *Phys. Lett. B* **697**, 32 (2011).  
 [8] B. Chen, Y. Liu, K. Zhou, and P. Zhuang, *Phys. Lett. B* **726**, 725 (2013).  
 [9] B. Chen, M. Hu, H. Zhang, and J. Zhao, *Phys. Lett. B* **802**, 135271 (2020).  
 [10] J. Zhao, K. Zhou, S. Chen, and P. Zhuang, *Prog. Part. Nucl. Phys.* **114**, 103801 (2020).  
 [11] A. Rothkopf, *Phys. Rep.* **858**, 1 (2020).  
 [12] F. Karsch, D. Kharzeev, and H. Satz, *Phys. Lett. B* **637**, 75 (2006).  
 [13] Y. Burnier, O. Kaczmarek, and A. Rothkopf, *J. High Energy Phys.* **12** (2015) 1.  
 [14] H. Satz, *J. Phys. G: Nucl. Part. Phys.* **32**, R25 (2006).  
 [15] M. E. Peskin, *Nucl. Phys. B* **156**, 365 (1979).  
 [16] D. Lafferty and A. Rothkopf, *Phys. Rev. D* **101**, 056010 (2020).  
 [17] Y. Burnier and A. Rothkopf, *Phys. Rev. D* **95**, 054511 (2017).  
 [18] B. Chen, *Chin. Phys. C* **43**, 124101 (2019).  
 [19] J. Zhao, B. Chen, and P. Zhuang, *Phys. Rev. C* **105**, 034902 (2022).  
 [20] J. P. Blaizot, D. De Boni, P. Faccioli, and G. Garberoglio, *Nucl. Phys. A* **946**, 49 (2016).  
 [21] B. Krouppa, R. Ryblewski, and M. Strickland, *Phys. Rev. C* **92**, 061901(R) (2015).  
 [22] J. Boyd, T. Cook, A. Islam, and M. Strickland, *Phys. Rev. D* **100**, 076019 (2019).  
 [23] R. Katz and P. B. Gossiaux, *Ann. Phys.* **368**, 267 (2016).  
 [24] S. Kajimoto, Y. Akamatsu, M. Asakawa, and A. Rothkopf, *Phys. Rev. D* **97**, 014003 (2018).  
 [25] L. Wen, X. Du, S. Shi, and B. Chen, *Chin. Phys. C* **46**, 114102 (2022).  
 [26] A. Islam and M. Strickland, *J. High Energy Phys.* (2020) 235.  
 [27] N. Brambilla, M. Á. Escobedo, M. Strickland, A. Vairo, P. Vander Griend, and J. H. Weber, *J. High Energy Phys.* **05** (2021) 136.  
 [28] Y. Akamatsu and A. Rothkopf, *Phys. Rev. D* **85**, 105011 (2012).  
 [29] Z. Xie and B. Chen, *arXiv:2205.13302*.  
 [30] X. Yao and T. Mehen, *Phys. Rev. D* **99**, 096028 (2019).  
 [31] X. Yao and B. Müller, *Phys. Rev. D* **100**, 014008 (2019).  
 [32] X. Yao and T. Mehen, *J. High Energy Phys.* **02** (2021) 62.  
 [33] M. Döring, S. Ejiri, O. Kaczmarek, F. Karsch, and E. Laermann, *Eur. Phys. J. C* **46**, 179 (2006).  
 [34] U. Kakade and B. K. Patra, *Phys. Rev. C* **92**, 024901 (2015).  
 [35] Y. Liu and B. Chen, *Chin. Phys. C* **44**, 124106 (2020).  
 [36] M. Tanabashi *et al.* (Particle Data Group), *Phys. Rev. D* **98**, 030001 (2018).  
 [37] K. Zhou, N. Xu, Z. Xu, and P. Zhuang, *Phys. Rev. C* **89**, 054911 (2014).  
 [38] A. Kadeer, J. G. Korner, and U. Moosbrugger, *Eur. Phys. J. C* **59**, 27 (2009).  
 [39] Z. Li, Y. Chen, D. Li, and M. Huang, *Chin. Phys. C* **42**, 013103 (2018).  
 [40] M. Laine, O. Philipsen, P. Romatschke, and M. Tassler, *J. High Energy Phys.* **03** (2007) 054.  
 [41] A. Dumitru, Y. Guo, and M. Strickland, *Phys. Rev. D* **79**, 114003 (2009).  
 [42] C. Shen and U. Heinz, *Phys. Rev. C* **85**, 054902 (2012); **86**, 049903(E) (2012).  
 [43] T. Hirano, *Phys. Rev. C* **65**, 011901(R) (2001).  
 [44] J. I. Kapusta and T. Toimela, *Phys. Rev. D* **37**, 3731 (1988).